(2)

CHEMICAL
RESEARCH,
DEVELOPMENT &
ENGINEERING
CENTER

CRDEC-TR-88071

FIBER OPTIC MICROSENSOR FOR RECEPTOR-BASED ASSAYS

Myron J. Block
Thomas R. Glass, Ph.D.

ORD, INC.
Nahant, MA 01908

James J. Valdes, Ph.D.

RESEARCH DIRECTORATE

September 1988

U.S. ARMY
ARMAMENT
MUNITIONS
CHEMICAL COMMAND

Aberdeen Proving Ground, Maryland 21010-5423

Disclaimer

The findings in this report are not to be construed as an official Department of the Army position unless so designated by other authorizing documents.

Distribution Statement

Approved for public release; distribution is unlimited.

UNCLASSIFIED

SECURITY CLASSIFICATION OF THIS PAGE

REPORT DOCUMENTATION PAGE

Form Approved OMB No. 0704-0188

1a. REPORT SECURITY CLASSIFICATION UNCLASSIFIED	1b. RESTRICTIVE MARKINGS
2a. SECURITY CLASSIFICATION AUTHORITY	3. DISTRIBUTION/AVAILABILITY OF REPORT Approved for public release; distribution is unlimited.
2b. DECLASSIFICATION/DOWNGRADING SCHEDULE	
4. PERFORMING ORGANIZATION REPORT NUMBER(S) CRDEC-TR-88071	5. MONITORING ORGANIZATION REPORT NUMBER(S)
6a. NAME OF PERFORMING ORGANIZATION ORD, Inc. — 6b. OFFICE SYMBOL (If applicable)	7a. NAME OF MONITORING ORGANIZATION
6c. ADDRESS (City, State, and ZIP Code) Nahant, MA 01908	7b. ADDRESS (City, State, and ZIP Code)
8a. NAME OF FUNDING/SPONSORING ORGANIZATION CRDEC — 8b. OFFICE SYMBOL (If applicable) SMCCR-RSB	9. PROCUREMENT INSTRUMENT IDENTIFICATION NUMBER DAAA15-86-C-0094
8c. ADDRESS (City, State, and ZIP Code) Aberdeen Proving Ground, MD 21010-5423	10. SOURCE OF FUNDING NUMBERS PROGRAM ELEMENT NO. — PROJECT NO. — TASK NO. — WORK UNIT ACCESSION NO.

11. TITLE (Include Security Classification)
Fiber Optic Microsensor for Receptor-Based Assays

12. PERSONAL AUTHOR(S)
Block, Myron J., Glass, Thomas R. (ORD); and Valdes, James J., Ph.D. (CRDEC)

13a. TYPE OF REPORT	13b. TIME COVERED	14. DATE OF REPORT (Year, Month, Day)	15. PAGE COUNT
Technical	FROM 86 Sep TO 87 Mar	1988 September	21

16. SUPPLEMENTARY NOTATION

17. COSATI CODES			18. SUBJECT TERMS (Continue on reverse if necessary and identify by block number)
FIELD	GROUP	SUB-GROUP	Microsensors; Receptor; Optical wave (, hd)
20	06		

19. ABSTRACT (Continue on reverse if necessary and identify by block number)

This project established the feasibility of adapting ~~ORD's~~ fiber optic fluorescence immunoassay (FFIA) instrument as a pocket-sized microsensor for rapid receptor-based assays. The instrument, with its light-emitting diode (LED) source and solid state detector, was demonstrated to satisfy projected sensitivity requirements for a receptor-based assay device. An aqueous solution of fluorescent tag was successfully detected at a noise equivalent concentration (NEC) in the subpicomolar range. In actual practice, system sensitivity will be limited by biological factors such as the ability of the receptor coating to specifically bind at such low concentrations.

20. DISTRIBUTION/AVAILABILITY OF ABSTRACT ☒ UNCLASSIFIED/UNLIMITED ☐ SAME AS RPT. ☐ DTIC USERS	21. ABSTRACT SECURITY CLASSIFICATION UNCLASSIFIED
22a. NAME OF RESPONSIBLE INDIVIDUAL SANDRA J. JOHNSON	22b. TELEPHONE (Include Area Code) (301) 671-2914 — 22c. OFFICE SYMBOL SMCCR-SPS-T

DD Form 1473, JUN 86 — Previous editions are obsolete. — SECURITY CLASSIFICATION OF THIS PAGE
UNCLASSIFIED

PREFACE

The work described in this report was authorized under Contract No. DAAA15-86-C-0094. This work was started in September 1986 and was completed in March 1987. Data are found in laboratory notebooks in the possession of the contractor.

The use of trade names or manufacturers' names in this report does not constitute an official endorsement of any commercial products. This report may not be cited for purposes of advertisement.

This report has been approved for release to the public.

Blank

CONTENTS

LIST OF FIGURES

LIST OF TABLES

Blank

FIBER OPTIC MICROSENSOR FOR RECEPTOR-BASED ASSAYS

1. AIMS AND OBJECTIVES

The objective was to determine the feasibility of adapting a fiber optic fluorescence immunoassay (FFIA) fluorometer to enable the development of a pocket size field instrument for receptor-based assays. The main obstacle to reducing the size of the instrument was the light source, a 5-W incandescent lamp. The power requirement for this lamp is not practical for a battery-operated, pocket-sized instrument, and dissipating the heat generated by this lamp without adversely affecting the performance of the instrument is difficult. We therefore proposed to use a red light-emitting diode (LED) as the light source in the instrument; these sources consume approximately 0.12 W, can easily be powered with batteries in a pocket-sized instrument, and are not plagued by heat dissipation. The feasibility of using an LED as the light source is determined by the sensitivity that can be achieved. Therefore, the goal of this research was to determine the sensitivity that can be achieved with an LED-based instrument.

a. Development of a computer model to analyze and compare the performance of different dye-LED combinations.

b. Use of the computer model to select the optimum filter specifications for each combination and to select the best dye-LED combination for further testing.

c. Modification of an instrument to use the selected components and evaluation of this modified instrument.

2. EXPERIMENTAL PROCEDURES AND CALCULATIONS

2.1 Computer Model.

The first step in the computer modeling effort was to identify candidate dye-LED combinations. A total of 13 dye-LED combinations derived from different pairs of five dyes and seven LEDs was identified. The dyes were phycobiliprotein dyes and were selected for their high fluorescent yield, high absorption coefficient, large stokes shift, ability to be conjugated, and because their absorption wavelength is compatible with LEDs. Table 1 lists the selected dyes with their characteristics. The seven LEDs and their characteristics are listed in Table 2. The computer model created for this contract was written in the ASYST programming language, a vector-oriented language ideal for working with arrays such as the spectral filter transmission and source power. The optical layout of the breadboard instrument is shown in Figure 1. This instrument is an epi-fluorometer using wavelength separation by interference filters to distinguish

fluorescence from reflected and scattered excitation. The variables in the computer model were the parameters of the LED source, the dye, and the filters.

Table 1. Dye Characteristics

Designation	Name	Absorption maximum (nm)	Emission maximum (nm)	Extinction coefficient	Quantum yield
B-PE	B-phycoerythrin	545	575	2,410,000	0.98
R-PE	R-phycoerythrin	565	578	1,960,000	0.68
C-PC	C-phycocyanine	620	650	1,690,000	0.51
A-PC	Allophycocyanine	650	660	700,000	0.68
R-PC	R-phycocyanine	555,618	634	760,000	0.70

Table 2. LED Characteristics

Designation	Type	Wavelength maximum (nm)	Rated output (μW)	Geometric coupling efficiency	Usable output (μW)
BG	GaP	555	9.4	0.106	1.0
PG	GAP	565	44	0.114	5.0
PY	GaP	570	83	0.066	5.5
AY	GaAsP	580	46	0.076	3.5
AA	GaAsP	605	31	0.051	1.6
AR	GaAsP	650	67	0.171	11.5
BR	GaAlAs	660	1870	0.255	477.0

The parameters for the LED source were its power spectrum and its geometric coupling efficiency. The power output spectrum for the LEDs was taken from the manufacturer's published data. The geometric coupling efficiency was the fraction of LED output power that can be coupled into the fiber, limited solely by geometric constraints. The geometric coupling efficiency differs for each type of LED (because of differences in size, shape, and emission pattern) and was experimentally determined for each LED type under consideration. This was done as shown in Figure 2. The pinhole simulated the fiber face, and the aperture restricted the angle of light entering the pinhole, to the maximum angle accepted by the fiber. The geometric coupling efficiency was the power through the pinhole, as measured by the detector diode, divided by the power output of the LED. Our results ranged from 0.051 to 0.255.

The parameters of the dye used by the computer model were the dye's absorbance and emission spectra, the extinction coefficient, and the quantum yield. All of these parameters were taken from the published data supplied by the manufacturer.

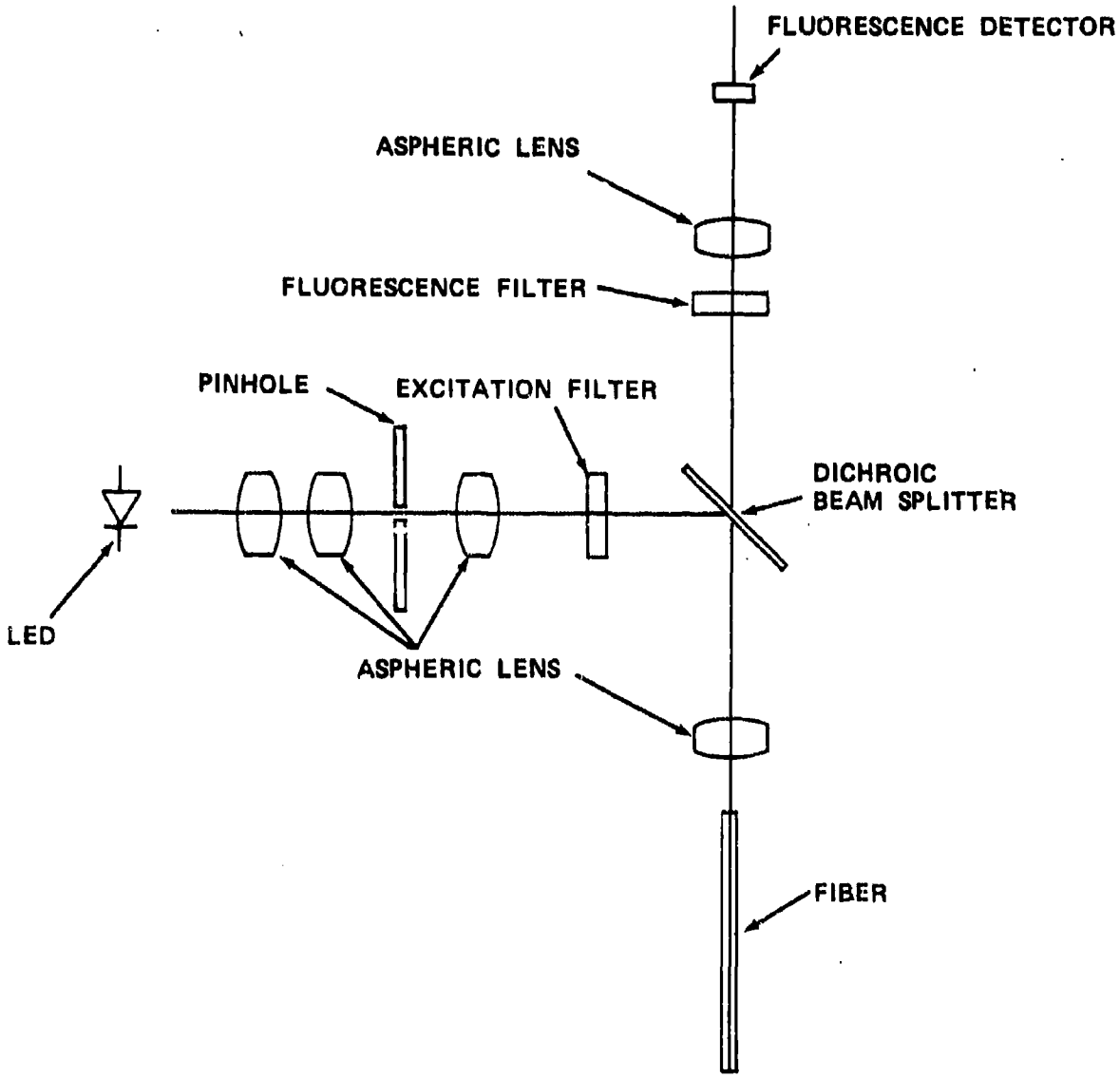

Figure 1. Optical Layout of Epi-Fluorometer

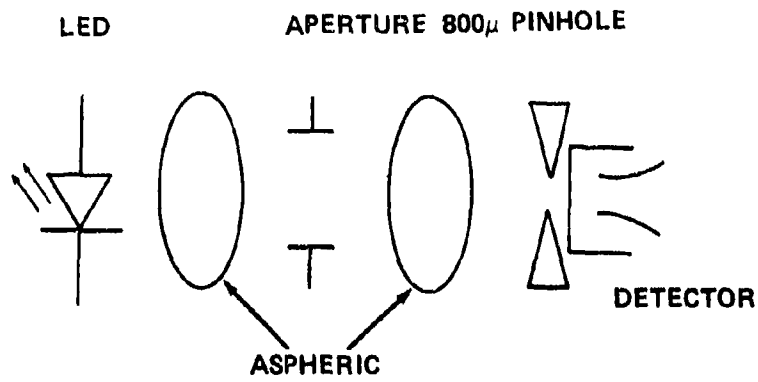

Figure 2. Schematic for Measuring Geometric Coupling Efficiency

The filters were completely specified by a spectral transmission curve. The model was programmed to generate this curve based on manufacturer's specifications from a given center wavelength and a passband width. This was done to allow the filter parameters to be put in as a range of values, which permitted the computer model to generate different filter curves as it stepped through the range.

2.2 Model Calculations.

The model calculated the signal-to-noise ratio for a given dye, LED, and filter set. The model could also act as an iterative calculator, in which case the signal-to-noise ratio was calculated for each filter set within a range of values and stored into an array. The highest signal-to-noise ratio could then be determined along with its corresponding filter values. In this way the model could be used to find the optimum filter parameters for a given dye-LED combination. In the present study, the computer model was used to select the optimum filter set for each of the 13 dye-LED combinations under consideration, and to rank order the 13 combinations according to the predicted signal-to-noise ratio of each combination. Table 3 shows a rank-order listing of the dye-LED combinations according to noise equivalent concentration (NEC) as computed by the model. The comparison factor number is used to compare different combinations. The comparison factor is the calculated signal-to-noise ratio, scaled so the lowest ranked combination has a value of one.

For the dye-LED combinations selected for further analysis, the computer model was used to make predictions of the instrument's performance based on the optimum filter sets previously selected. Predictions were made of the excitation power into the fiber, the background level from a clean dry fiber, and the signal level from a dye sample.

Table 3. Predicted Signal-to-Noise Ratios for Dye-LED Combinations

Rank	Dye	LED	Comparison factor
1	A-PC	BR	336
2	C-PC	BR	100
3	C-PC	PY	27
4	C-PC	PG	24
5	R-PE	PG	20
6	R-PC	PY	18
7	R-PC	PG	17
8	B-PE	BG	13
9	A-PC	PY	7.5
10	A-PC	AR	7
11	R-PE	BG	6
12	A-PC	AA	5.5
13	R-PC	AY	1

2.3 Modification and Evaluation of the Instrument.

The top two dye-LED combinations, rather than just the top one as proposed, were used to evaluate the instrument. This was necessary for proper verification of the model's accuracy because the model was intended to calculate only the relative change in signal for various combinations, rather than the absolute signal level. Modification of one of the existing FFIA instruments included redesigning the optical system and installing the filter set selected by the computer model. The optical system was designed for best imaging of the LED onto the fiber proximal face, bearing in mind the numerical aperture of the fiber. Using off-the-shelf lenses, a magnification of one is best. This is backed up by our experimental evaluation of the geometric coupling efficiency for diodes where the most efficient transfer occurred for unit magnification. Figure 3 shows the optical design.

Evaluation of the instrument was done with both A-phycocyanine (A-PC) and C-phycocyanine (C-PC) filter sets and dyes, the LED being the same for both. The first test was to measure the excitation power delivered to the fiber. This was done by putting a pinhole at the focus of the objective lens to simulate the fiber face and measuring the power through the pinhole (Figure 4). For both combinations, the measured power was slightly lower than the calculated power. In the case of the A-PC filter set, the calculated power was 214 μW while the measured power was 168.1 μW, a difference of 21.5%. For the C-PC filters, the calculated power was 92 μW and the measured power was 81.1 μW, a difference of 11.8%. These values show reasonable agreement with the computer model's predictions. The second test

was the comparison of background levels, background being the detector reading measured from a clean, dry fiber. The measured background levels were higher than the calculated levels. For the A-PC filter set, the calculated reading was 160 mV and the measured reading was 242 mV, a 51% increase from the calculated value. The C-PC filter set measurements were 74 mV calculated and 178 mV measured, a reading 141% higher than calculated.

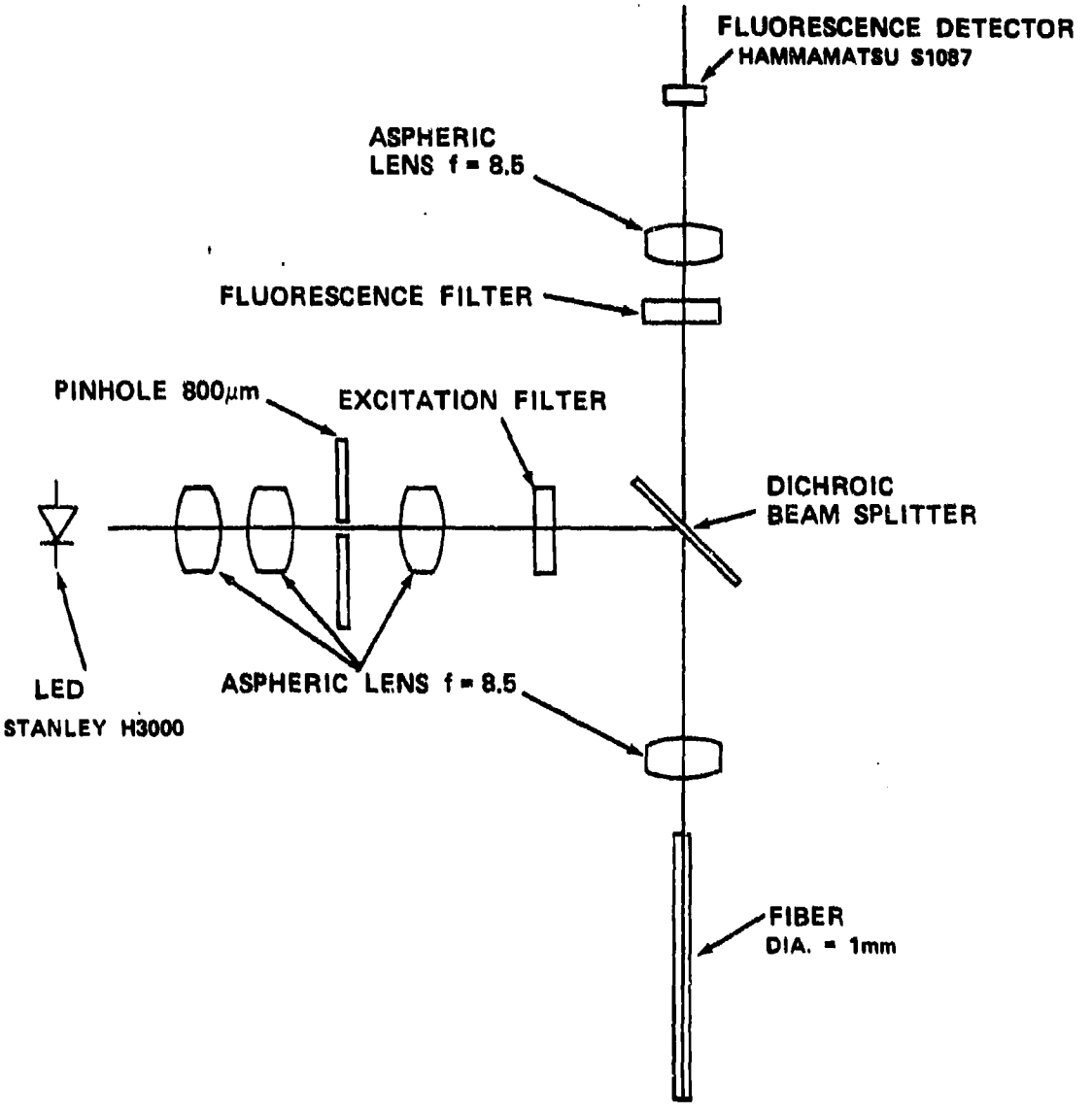

Figure 3. Modified FFIA Instrument

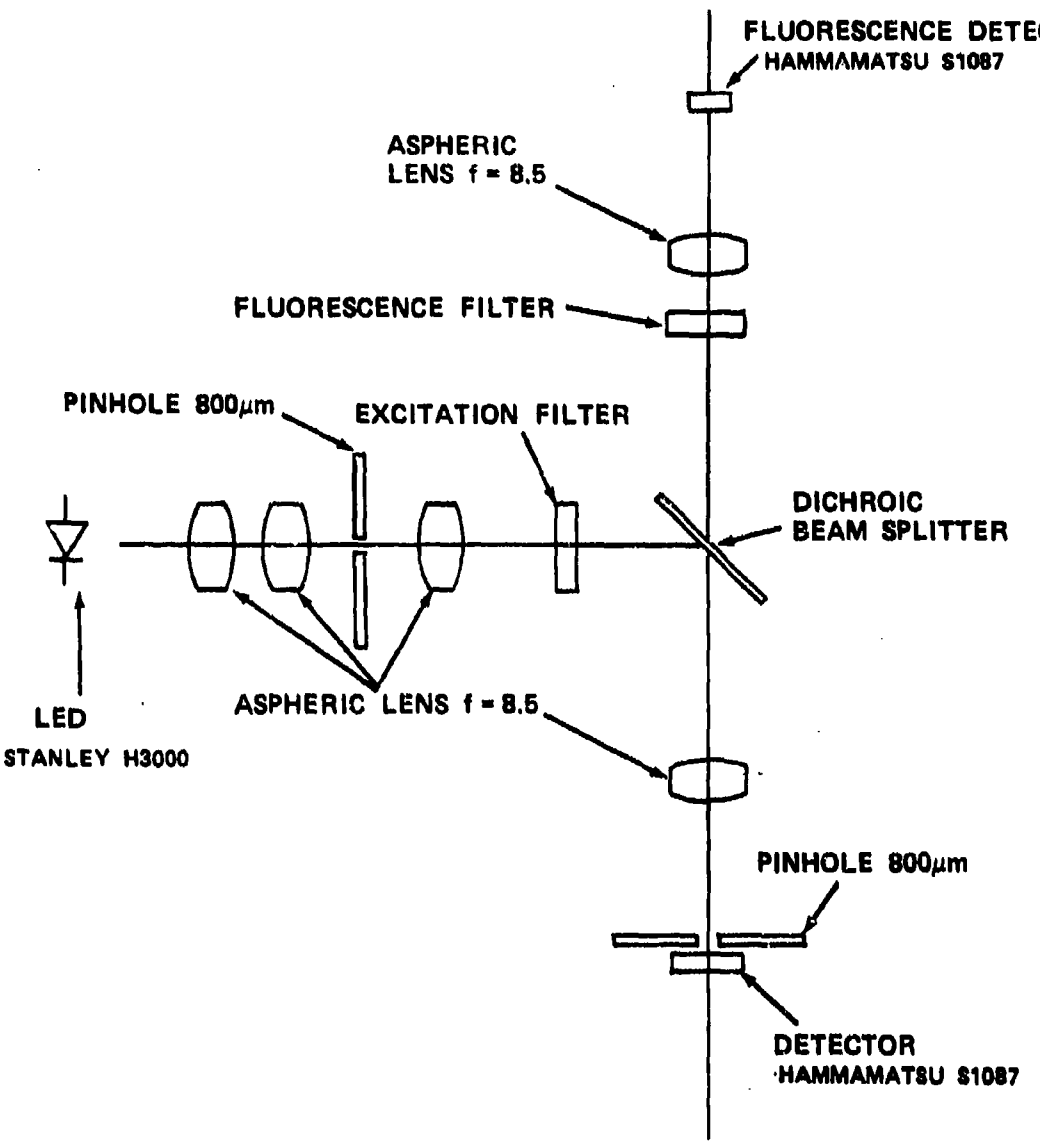

Figure 4. Test Instrument for Measuring Excitation Power Delivered to Fiber

The last measurement for comparison to the computer model's predictions was the relative sensitivity between A-PC and C-PC dye. The measurements were made with 10^{-7} molar concentration of dye surrounding approximately 25 mm of fiber. The signal value used was the average of several readings, nine readings for A-PC dye and six readings for C-PC. The signal for A-PC was 2.41 V and the signal for C-PC was 1.53 V. The relative sensitivity was calculated as the A-PC signal-to-noise ratio divided by the C-PC signal-to-noise ratio. Since the noise is the same

for both the A-PC and the C-PC signals, the ratio of signal to noise for the two dyes was simply the ratio of the signals. The computer model predicted this ratio to be 3.36 (A-PC over C-PC), but the measured value was 1.58, a factor of 2.1 lower than predicted. Although the measured ratio was lower than the predicted ratio, it was close enough to show that the computer model's prediction was reasonably accurate.

C-PC dye was used for the demonstration of the NEC achievable with an LED-based instrument because of drift noticed with an A-PC filter set. NEC was defined as the concentration of dye that gives rise to a signal equal to the instrument noise. This is calculated by linear extrapolation using a known concentration of dye that gives a signal well above the instrument noise. For the C-PC dye, an aqueous dye concentration of 1×10^{-9} molar gave a signal of 0.94 V. Since the instrument noise was 0.5 mV, a nanomolar concentration of dye yields a signal-to-noise ratio of 1880. The signal was directly proportional to the concentration of dye, yielding a calculated NEC of 5.3×10^{-13} molar.

2.4 Problems Encountered and Their Solutions.

The optimum filter sets chosen by the computer model were not readily available. Therefore, the nearest available filters were chosen and these values were checked with the computer model. The model showed that these results were only a few percent lower than the optimum sets (Table 4). During the readings, the values obtained with the A-PC filter set decreased with time as a result of LED self-heating. The output spectrum of the LED shifted to longer wavelengths as the LED temperature increased. Since the excitation filter only passes the shorter wavelengths of the LED output, the excitation power at the fiber decreased as the LED heated. This effect is much more pronounced for the A-PC than for the C-PC filter set because the A-PC excitation filter passband is closer to the peak output of the LED, so that a shift in output spectrum of the LED caused a larger change in transmitted power. In practice, this problem could be avoided by devising a better method of heat sinking the LED. To avoid the drift seen with the A-PC filters, the LED was run at 1-mA drive current instead of the 50-mA normally used. This change in drive current changed the magnitude of the signals, but did not change the relative signal readings between the two dyes. The fact that the background is higher than calculated, while the excitation power is lower than calculated, showed the computer model to be incomplete in this respect. The background spectrum would need to be measured to determine if the higher readings were caused from a higher reflection than the 4% assumed, if there was a shift in the wavelength from fluorescence, or a possible Raman shift in the fiber.

Table 4. Comparison of Optimum to Actual Signal-to-Noise Ratios

	Excitation filter		Fluorescence filter		Dichroic cutoff wavelength	Percentage of decrease in S/N optimum to actual
	Continuous wave	Bandwidth	Continuous wave	Bandwidth		
A-PC						
Optimum	650	40	720	50	685	4.2
Actual	646	40	724	58	690	
C-PC						
Optimum	630	40	710	60	665	5.0
Actual	630	37	720	60	665	

2.5 Calculations Required for Complete Definition.

The geometric coupling efficiency is the power through the pinhole, as measured by the detector diode, divided by the power output of the LED. Results ranged from 0.051 to 0.255. The calculations were performed by the model in the following manner. The model computed the fluorescent signal by multiplying the source power spectrum by the source geometric coupling efficiency, the transmission curve of the excitation filter, the spectral reflection of the dichroic, and the spectral absorbance characteristics of the dye. The resulting product was integrated over wavelength to determine an "effective" excitation power. The total power of the fluorescent response was proportional to the integrated excitation power. The constant of proportionality took into account such factors as dye concentration, the active area of the fiber, the efficiency of coupling excitation light to the dye, and the efficiency of the emitted fluorescence tunneling back into the fiber. The weighted fluorescent response (i.e., the signal spectrum) was then multiplied by the spectral transmission curve of the dichroic, the fluorescence filter, and the spectral sensitivity of the detector. The integral over wavelength of the resulting distribution was the predicted signal output of the system.

This was only half of the task, however. Before the model could predict sensitivity, it also had to calculate system noise that has two components: detector noise, which is fixed for a given detector, and shot noise of background, which must be computed from the background leakage for each filter set. The principal contributor in leakage of excitation to the detector is Fresnel reflection from the fiber proximal face. Therefore, for

modeling purposes, an assumption was made for reflection of 4% of the excitation power at the fiber face, followed by application of the same computation (i.e., filtering through the dichroic and fluorescence filter) that was applied to fluorescence exiting the fiber to get background. From this, a noise value was calculated and a signal-to-noise ratio was determined.

2.6 Evanescent Penetration Distance.

The following is a calculation performed to quantify the penetration depth. The calculation essentially confirmed the previous assumption that the evanescent penetration depth is approximately 1/5 of the wavelength used. The calculation also gave additional insight into factors controlling the penetration depth. The starting point was an equation* for the electric field amplitude in the evanescent zone,

$$E = E_o \exp-\left[\frac{2\pi\left(\sin^2\Theta - n_{21}^2\right)^{1/2} x}{\lambda}\right]$$

where x is the distance from the fiber and Θ is measured from a normal to the fiber surface. E_o is the incident electric field amplitude inside the fiber. From basic radiometry** we know that E_o is also angle dependent, given by,

$$E_o^2 \propto \cos\alpha \sin\alpha$$

where α is the complimentary angle to Θ. We can now write the expression for the total electric field intensity in the evanescent zone as

$$E^2 \propto \sin\alpha \cos\alpha \left\{\exp-\left[\frac{2\pi\left(\cos^2\alpha - n_{21}^2\right)^{1/2} x}{\lambda}\right]\right\}^2$$

In our specific case, the fiber core was filled to its maximum NA. In this case, the excitation was proportional to the integral of E^2 (given above) from 0 to α_{max}, where

$$\alpha_{max} = \sin^{-1}\left(\frac{\sqrt{n_1^2 - n_2^2}}{n_1}\right)$$

*Harrick, N.J., Internal Reflection Spectroscopy, Interscience Publishers, New York, NY, 1967.

**Boyd, R.W., Radiometry and the Detection of Optical Radiation, John Wiley & Sons, New York, NY, 1983.

Because this system detects all the fluorescence that exits from the fiber's proximal face, it is not necessary to include the sin α cos α term in the collection efficiency, so

$$E_o \propto \left\{ \exp- \left[\frac{2\pi\left(\cos^2 \alpha - n_{21}^2\right)^{1/2} x}{\lambda} \right] \right\}^2$$

which again must be integrated from 0 to α_{max}. We have performed the integrations, multiplied the excitation and collection terms, and plotted the results. Figure 5 shows a family of curves, each corresponding to a different core index. The y axis is the relative signal level and the x axis is the distance from the fiber. Notice that if one assumes that the curves are exponentials, which is not the case, and calculates the 1/e point for each one, the "penetration depth" would increase as n_{21} decreases. That is, the lower core index would give a larger 1/e distance. In fact, however, the signal increased with increasing n_{21}. Figure 6 shows the same family of curves plotted as a three-dimensional surface.

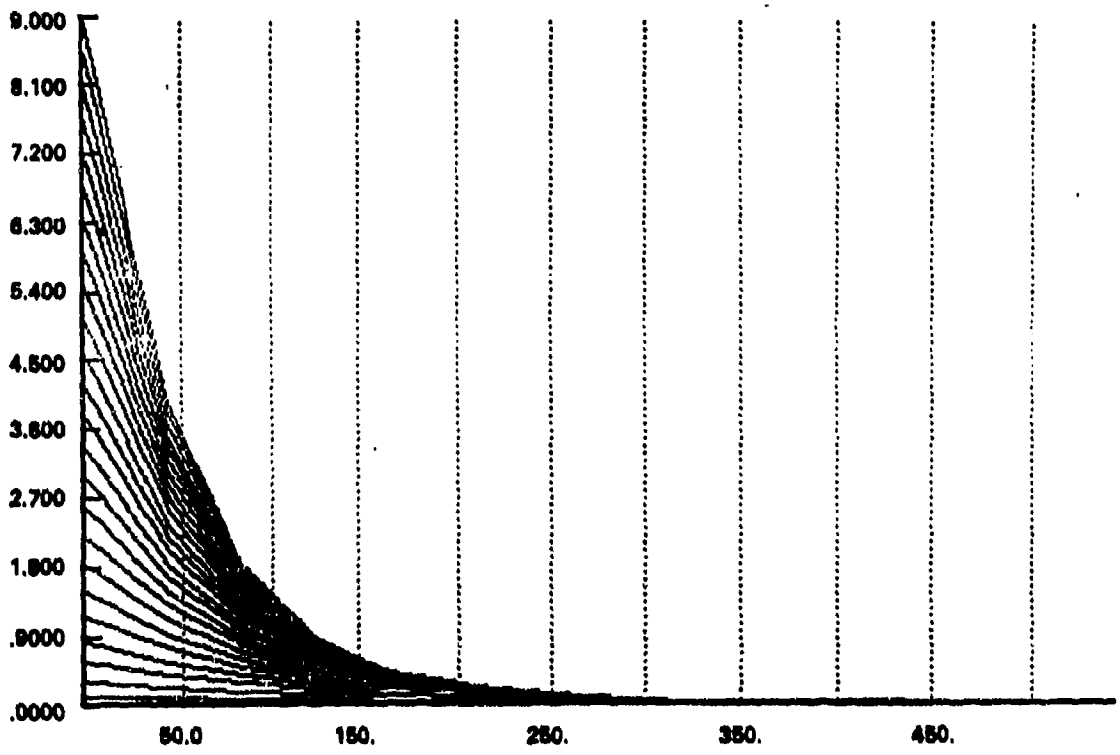

Figure 5. Signal vs. Distance from Fiber with Increasing N_1

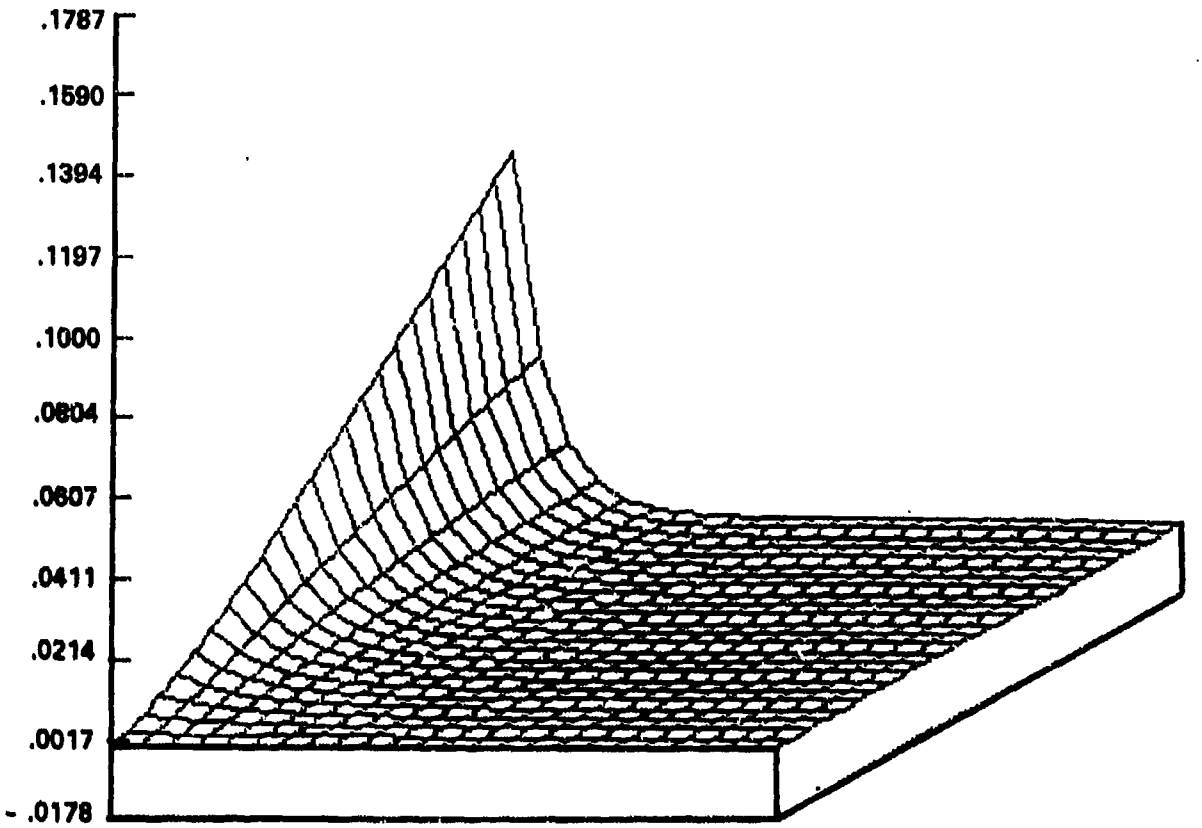

Figure 6. Signal as a Function of Distance and Index

In Figure 7, the factor of increase in signal was plotted as a function of distance from the fiber for three different cases: One case involved changing only the core index (2:1), another involved changing only the wavelength (3:1), and the third involved both (4:1).

3. CONCLUSIONS

The data established the feasibility of adapting a FFIA instrument as a pocket-sized microsensor for rapid receptor-based assays. A briefcase-sized version of the instrument was modified to incorporate components such as an LED source and solid state detector suitable for use in a pocket-sized instrument. This modified instrument was then demonstrated under laboratory conditions to satisfy projected sensitivity requirements for a receptor-based assay device.

This demonstration employed a red LED and C-phycocyanine (C-PC), a prospective fluorescent label for receptor-based assays. The instrument successfully detected an aqueous solution of fluorescent tag at an NEC in the subpicomolar range. We defined NEC as the concentration at which the signal-to-noise

ratio equals 1, for a 1-Hz bandwidth. At this NEC, there were about 3,500 fluorescent molecules in the evanescent zone of the fiber. For a fiber surface coating that can bind all the fluorescently labeled moiety in the capillary tube surrounding the fiber, this translates to a receptor-based detection sensitivity in the subfemtomolar range. Of course, this only represents the sensitivity of our optical transducer system, and in actual practice system sensitivity will be limited by biological factors (e.g., the ability of the receptor coating to specifically bind at such low concentrations). A computer model was developed to guide selection of the combination of LED and fluorescent dye. The two most efficient combinations were installed in an instrument optimized for those particular combinations, and the performance of each combination was evaluated.

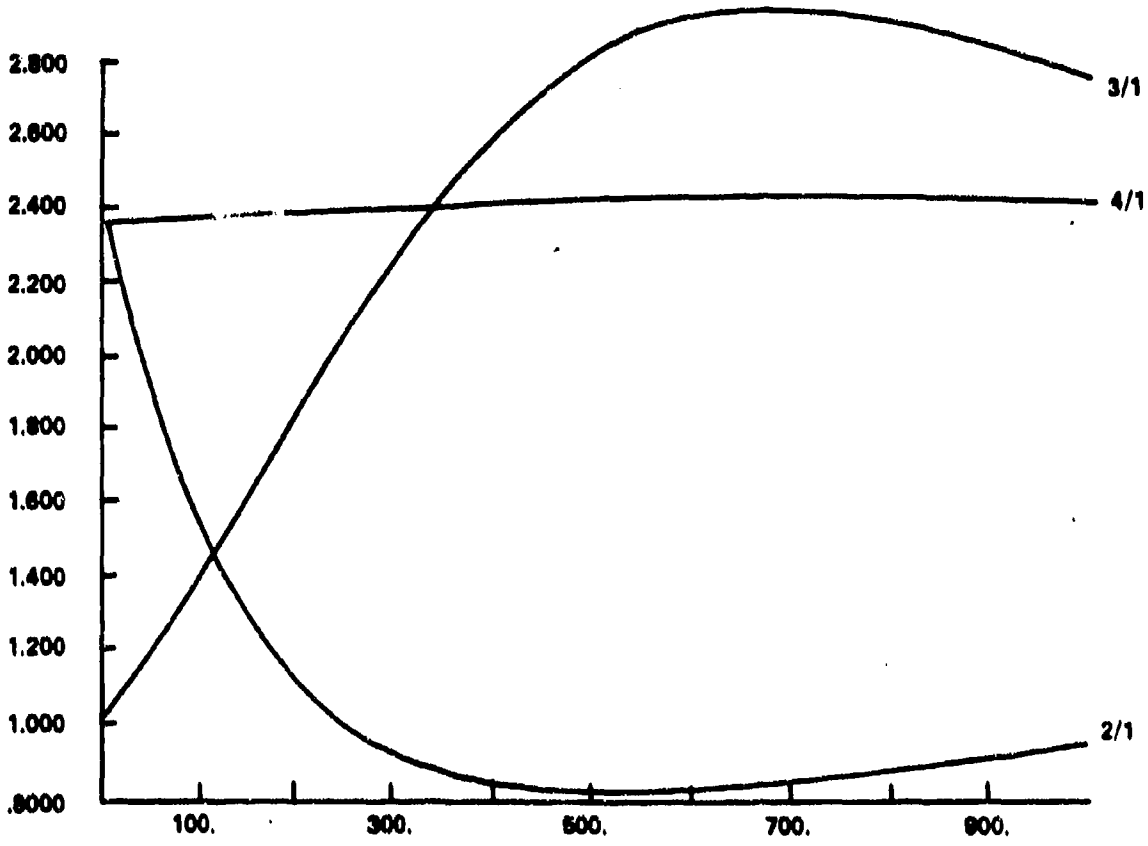

Figure 7. Signal as a Function of Distance from the Fiber

A theoretical analysis of evanescent penetration distance and the factors affecting it was also performed. This increased our understanding of the fundamental physics of the phenomena applicable to the development of a receptor-based biosensor. While not perfect, the computer model proved sufficiently accurate to select the best available dye-LED combination from the list of candidates. The sensitivity achieved in this phase I effort was a NEC of 5.3×10^{-13} molar. Although this sensitivity was better than the presently anticipated need, several possibilities for improving it further have been identified. The analysis of evanescent penetration distance showed that the 1/e point of the evanescent field was about 100 nm from the surface of the fiber. Since the size of the receptor is typically <30 nm, any assay format will hold the bound fluorophore well within the 100-nm evanescent zone.

This sensitivity was achieved with the LED operating continuously at room temperature. The LED source, in addition to its advantages over an incandescent lamp in size and efficiency, has other characteristics that can be exploited in order to increase the instrument's sensitivity. For example, the LED can be pulsed to a peak intensity about 10 times brighter than its continuous output value without adversely affecting its life or performance. This pulsing can be exploited in two ways. One way is to read the detector output only during the pulse, which increases the excitation intensity and thus the sensitivity. Another possibility with a pulsed source is time-resolved fluorescence, in which the reflected and scattered light are separated in time from the emitted fluorescence. Separating the fluorescent signal from the reflected and scattered excitation by this method would allow the filters that normally separate excitation from fluorescence to be made to pass a much wider spectrum, or even to be eliminated altogether. This would allow a much higher percentage of the source power to excite the sample and allow much more of the emitted light to reach the detector, thus improving sensitivity.

Another characteristic of the LED is that its output spectrum can be shifted by changing its temperature. The LED evaluated was the Stanley H-3000, which has its peak intensity at 660 nm at room temperature, a longer wavelength than the peak absorbance of the dyes used. Because of this, at room temperature (the conditions of the LED during the experiments), the output power of the LED could not be efficiently used. Cooling the LED would shorten the emission wavelength and increase light output of the LED, both of which are desirable. A shorter emission wavelength from the LED will allow much more output power of the LED to pass through the excitation filter, thereby increasing excitation power to the sample and thus improving sensitivity.

All the above methods would increase complexity as well as sensitivity. These methods are available, but at present are not necessary due to the specific binding capability of

receptors. With the methods available to improve sensitivity, instrument sensitivity will not become a limiting factor.

Because of its size, sensitivity, and speed, a pocket-sized fiber optic instrument would be ideal for infield, real-time, receptor-based assays. By simply using a fiber optic with a different coating this same instrument could also be used for any antibody-based assay. Since the coating on the fiber dictate what testing can be done, this pocket size instrument could be used with a stock of appropriate fibers for a very wide range of applications, including infield chemical and biological warfare testing, on-the-spot immunoassays by medical personnel, or even tests for drugs of abuse with the advantage of yielding immediate results.

Nonmilitary uses could be just as diverse. Its small size and its speed would make this instrument valuable to emergency medical personnel, because its rapid response could guide the correct course of action in a life-threatening situation. The instrument's speed and sensitivity would be a great improvement over present hospital methods. Since sample preparation is unnecessary, its use in doctors' offices would also be practical. Its small size, battery operation, and speed would make this instrument valuable for screening blood donors before, rather than after donations are taken, thus saving time and material. Drug testing could also be very useful in the nonmilitary market.